nature neuroscience

ARTICLES

# Sip1 regulates sequential fate decisions by feedback signaling from postmitotic neurons to progenitors

Eve Seuntjens[1,2,5], Anjana Nityanandam[3,5], Amaya Miquelajauregui[3], Joke Debruyn[1,2], Agata Stryjewska[1,2], Sandra Goebbels[3], Klaus-Armin Nave[3], Danny Huylebroeck[1,2] & Victor Tarabykin[3,4]

**The fate of cortical progenitors, which progressively generate neurons and glial cells during development, is determined by temporally and spatially regulated signaling mechanisms. We found that the transcription factor Sip1 (Zfhx1b), which is produced at high levels in postmitotic neocortical neurons, regulates progenitor fate non–cell autonomously. Conditional deletion of Sip1 in young neurons induced premature production of upper-layer neurons at the expense of deep layers, precocious and increased generation of glial precursors, and enhanced postnatal astrocytogenesis. The premature upper-layer generation coincided with overexpression of the *neurotrophin-3* (*Ntf3*) gene and upregulation of *fibroblast growth factor 9* (*Fgf9*) gene expression preceded precocious gliogenesis. Exogenous application of Fgf9 to mouse cortical slices induced excessive generation of glial precursors in the germinal zone. Our data suggest that Sip1 restrains the production of signaling factors in postmitotic neurons that feed back to progenitors to regulate the timing of cell fate switch and the number of neurons and glial cells throughout corticogenesis.**



A single layer of neuroepithelial cells lining the embryonic neural tube gives rise to the entire repertoire of neurons, astrocytes and oligodendrocytes of the adult CNS. Early in development, some progenitors of the cortical ventricular zone are multipotent and can generate both projection neurons and astrocytes. Later, precursor cells tend to become more lineage restricted[1–4]. In mice, the generation of cortical projection neurons and glia starts at embryonic day 11.5 (E11.5) and follows a temporally specified sequence of cell commitment and differentiation *in vivo* and *ex vivo*[5,6]. Following an inside first–outside last pattern of cortical lamination, neurons of deep layers 6 and 5 are generated before the molecularly and functionally distinct neurons of upper layers 4, 3 and 2. The time of birth of a neuron can be used to accurately predict its laminar fate[5,7].

The intrinsic and extrinsic factors controlling the progressive restriction in developmental potential and the ultimate fate of cortical progenitors have not been completely elucidated[4,8,9]. Early cortical progenitors, when cultured *in vitro*, generate different cortical cell types in a sequence that recapitulates neurogenesis *in vivo*, suggesting the existence of an inherent genetic program[8]. Furthermore, there are indications that feedback mechanisms involving young neurons might act to restrict precursor cells from producing more of their own type[4,9].

*Sip1* was identified as a gene whose expression is upregulated in postmitotic neurons of the embryonic neocortex (V.T., unpublished data). Sip1 is a DNA-binding transcriptional repressor that interacts with activated Smads, the transducers of TGFβ signaling[10], and with the NuRD complex[11]. It also activates transcription on association with Smad8 (ref. 12). Several types of mutations in *ZFHX1B* (also known as *ZEB2*) cause Mowat-Wilson syndrome, which is characterized by mental retardation, microcephaly and distinct facial malformations[13].

*Sip1* knockout mice die at E9.5, fail to close the neural tube, lack vagal neural crest cells and show defective migration of cranial neural crest cells[14]. To investigate the function(s) of *Sip1* in the developing neocortex (beginning at E11.5), we analyzed *lox*P/Cre-based conditional knockout mice. We deleted *Sip1* in either the entire mouse CNS (using a *Nestin-cre* approach), dorsal telencephalic precursors (*Emx1-cre*) or dorsal telencephalic postmitotic cells (*Nex-cre*)[15–17]. We found that specific ablation of *Sip1* in the neocortex led to a temporal shift in corticogenesis, mediated by premature feedback signaling from cortical plate neurons to progenitor cells via *Ntf3* and *Fgf9*. It seems that the fate of cortical progenitor cells is not only determined intrinsically, but is also influenced by the environment created by postmitotic neurons.

## RESULTS

### Sip1 levels are high in postmitotic neocortical cells

*Sip1* transcripts are detected at the onset of neurogenesis in the postmitotic cells of the mouse neocortex, with barely detectable levels in progenitors[18]. By immunohistochemistry, we found high Sip1 protein levels in the cortical plate, but none in progenitors (**Fig. 1a–c**). In the medial/cingulate cortex, the Sip1 domain at late gestation (E18.5) became restricted to cells of the deep layers (**Fig. 1c**).

We deleted *Sip1* using three different *cre* strains crossed to mice in which the critical exon 7 of *Sip1* is flanked by *loxP* sites[19]. We used *Nestin-cre* to inactivate *Sip1* in the entire CNS (**Fig. 1d**) and

[1]Laboratory of Molecular Biology (Celgen), Centre for Human Genetics, KULeuven, Leuven, Belgium. [2]Department of Molecular and Developmental Genetics (VIB11), Flanders Institute for Biotechnology, Leuven, Belgium. [3]Max-Planck-Institute for Experimental Medicine, Göttingen, Germany. [4]Institute of Cell Biology and Neurobiology Charité–Universitätsmedizin Berlin, Campus Mitte, Berlin, Germany. [5]These authors contributed equally to this work. Correspondence should be addressed to D.H. (danny.huylebroeck@med.kuleuven.be) or V.T. (tarabykin@em.mpg.de).

Received 24 June; accepted 25 August; published online 18 October 2009; doi:10.1038/nn.2409

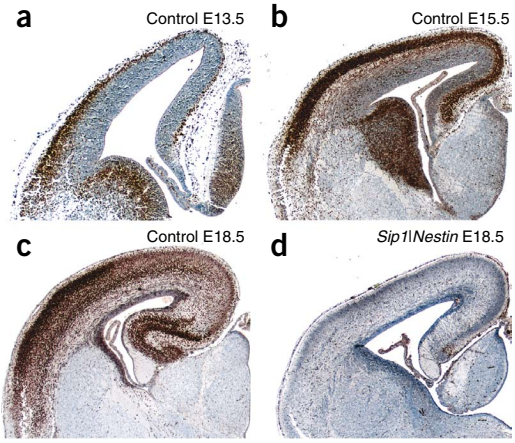


**Figure 1** Expression of Sip1 in the embryonic neocortex. (**a**) Sip1 immunostaining at E13.5 was found in the ventricular zone of the ventral telencephalon and in the postmitotic cells of the neocortex. (**b**) At E15.5, Sip1 expression was intense in the postmitotic cells of the neocortex, where invading Sip1-positive cells from the ventral telencephalon could be seen as well. (**c**) At E18.5, Sip1 synthesis was area specific; in the lateral neocortex, it was maintained in the entire cortical plate, whereas it was downregulated in the upper layers of the cingulate cortex. (**d**) Conditional knockout of *Sip1* (shown here using *Nestin-cre*) resulted in the almost complete loss of Sip1 protein from the neocortex and the ventral telencephalon.

*Emx1-IRES-cre* to ablate *Sip1* exclusively in neocortical progenitors starting from E9.5 (refs. 15,17). To separate *Sip1*'s function in early cortical progenitor cells from its role in postmitotic neurons, we used a *Nex-cre* approach. Previous studies have found that the majority of cells that produce Cre driven by the *Nex* promoter are nondividing neurons, whereas only a very small fraction are proliferative[16,20]. Moreover, immunostaining of *Nex*-driven Cre and neuronal HuC/D in the neocortex showed an almost complete overlay of both at E14.5 (**Supplementary Fig. 1**). Hence, in $Sip1^{loxP/-}$; *Nex-cre* mice (referred to here as *Sip1*|*Nex* mice), Cre was synthesized almost exclusively in postmitotic neurons and not in progenitor cells, specifically deleting *Sip1* in the differentiating field of the neocortex. Mutant mice are $Sip1^{loxP/-}$; *Nestin-cre* (*Sip1*|*Nestin*), $Sip1^{loxP/loxP}$; *Emx1-cre* (*Sip1*|*Emx1*) and *Sip1*|*Nex*; control littermates are referred to as such. We determined the efficiency of *Sip1* deletion in all three models. At E18.5, most neocortical cells in *Sip1*|*Emx1*, *Sip1*|*Nex* and *Sip1*|*Nestin* embryos no longer contained Sip1 (**Fig. 1d** and **Supplementary Fig. 1**). *Sip1*|*Nestin* mice died at birth, whereas both *Sip1*|*Emx1* and *Sip1*|*Nex* mice survived until 3–4 weeks after birth. Notably, the neocortical phenotype (see below) observed in all three models was nearly identical.

## Lack of Sip1 causes premature generation of upper layers

We checked whether the absence of Sip1 affects the specification of various neuronal cell types in the neocortex. We immunostained cortices for layer-specific markers (Tbr1 for layer 6, Ctip2 for layer 5 and Satb2 or Brn2 for layers 2–4) and calculated the proportions of the different cell types they labeled at E18.5 (**Fig. 2**). The number of deep-layer cells was reduced (layer 5: 10.6% in *Sip1*|*Nestin* and 12% in *Sip1*|*Nex* versus 21.1% and 19.3% in their respective controls; layer 6: 27.9% in *Sip1*|*Nestin* and 20% in *Sip1*|*Nex* versus 41.8% and 43.7% in their respective controls), whereas the upper layers (2–4) expanded (61.5% in *Sip1*|*Nestin* and 68.1% in *Sip1*|*Nex* versus 37.1% and 37% in their respective controls) (**Fig. 2h**). Populations of cells marked by Sox5 and Foxp2 were reduced as well (data not shown), implying that *Sip1* deletion affected the proportion of neuronal cell types and not just expression of certain markers. In addition, although the proportion of cell types had changed, their relative position in the neocortex remained largely unperturbed (**Fig. 2a–f**).

Because upper layers seem to have expanded at the expense of deep layers in mutant embryos, we investigated whether cortical neurons were generated in the correct time frame and in the right temporal sequence in the absence of Sip1. To determine the birthdates of layer-specific neurons, we labeled mitotically active precursors with BrdU (intraperitoneal injections into pregnant females) at different stages of embryogenesis (E11.5, 12.5, 13.5 and 15.5) and immunostained the cortices (E18.5 or postnatal day 2, P2) for both BrdU and a layer-specific marker. We calculated the percentage of layer-specific cell types born at the time of injection (percentage of BrdU-positive and marker-positive cells per total number of marker-positive cells). This analysis revealed that the peaks of production of Ctip2-positive layer 5 neurons and Brn2-positive layer 2–4 cells had shifted to 1 d earlier in Sip1 mutants (**Fig. 3a**,**b**). The generation of Tbr1-positive layer 6 neurons, however, remained unchanged (**Fig. 3a**). In the *Sip1*|*Nestin* neocortex, twice as many Ctip2-positive layer 5 neurons were born at E12.5 (16.6% in the mutant versus 7.6% in the control) and 50% more Brn2-positive layer 2–4 cells were generated at E13.5 (19.3% in mutant versus 12.8% in control), whereas 70% more Ctip2-positive cells (30.5% versus 17.8%) and 2.5-fold more Brn2-positive upper-layer cells (13.2% versus 5.2%) were generated at E12.5 in *Sip1*|*Nex* mice when compared with the control (**Fig. 3a**,**b**). At E15.5, only half the number of layer 2–4 neurons were generated in the mutant neocortex (4.8% in *Sip1*|*Nestin* versus 11.4% in control), suggesting that neurogenesis might be ending prematurely (**Fig. 3a**). Moreover, the reduction in layer 5/6 neurons was already evident at E14.5, which coincided with the precocious appearance of Brn2 and Satb2 double-positive cells in the mutant cortical plate (**Fig. 3c–e** and data not shown). We ruled out apoptosis as a cause of depletion of deep-layer neurons, as we found no differences in the number of cells harboring cleaved caspase-3 between control and mutant neocortex from E13.5 to E17.5 (data not shown). We also found no differences in the expression of the postmitotic neuronal marker HuC/D at E12.5 (data not shown). Together with the unaffected pattern of layer 6 generation (based on the specification of Tbr1-positive cells at E11.5–13.5 from BrdU pulse-chase experiments; **Fig. 3a**), this suggests that the onset of neurogenesis in *Sip1* conditional mutants was not altered. However, once neurogenesis commences, the timing of production of different cell types was shifted to earlier stages of development, irrespective of the number of each type generated.

The precocious determination of early cortical progenitors toward later cell types could be a result of shortened cell cycle of early progenitors, depletion of progenitor pool resulting from accelerated mitotic exit or a direct influence on cell fate determination of progenitor cells at a certain stage of neurogenesis. A shortening of the cell cycle would lead to an acceleration of the intrinsic clock and consequently premature generation of late-born neuronal layers. However, we found no differences in the cell-cycle length between control and mutant brains at E12.5 (**Supplementary Fig. 2**). A second possibility would be accelerated mitotic exit of early progenitor cells, which would lead to a depletion of their pool and, in turn, result in fewer early-born neurons. Once again, we found no substantial difference in the proportion of cells quitting the cell cycle at E12.5 (**Supplementary Fig. 2**). Furthermore, on the basis of Ki67 staining, M-phase markers phospho-histone3 (PH3) and radial glial marker phospho-Vimentin (pVim), we detected no differences in the extent of proliferation from E12.5–16.5 in mutant cortices (data not shown). We therefore

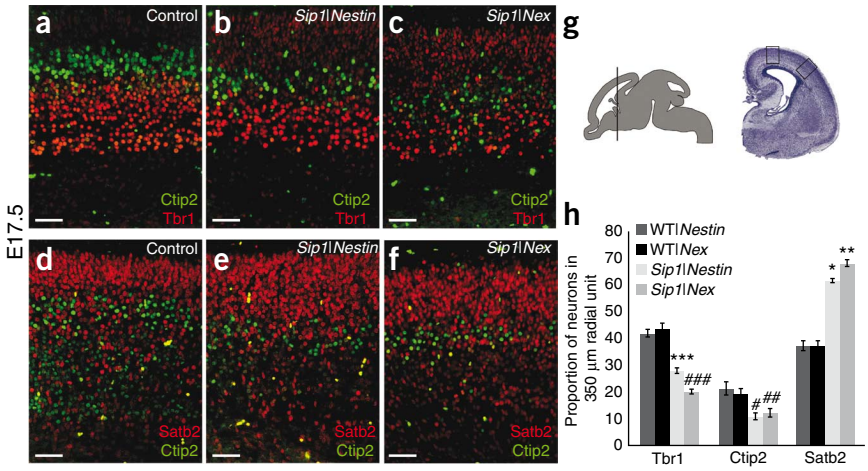


**Figure 2** Sip1-deprived neocortex contains excessive numbers of upper layer neurons at the expense of deep layer neurons whilst maintaining their relative position within the neocortex. (**a**–**c**) Double immunolabeling for Tbr1 (layer6) and Ctip2 (layer5) showed a reduction of deep layers when Sip1 was removed from either the entire brain (*Sip1|Nestin*; **b**) or postmitotic neurons (*Sip1|Nex*; **c**). (**d**–**f**) Double labeling of Satb2 (layers 2–4) and Ctip2 showed increased size of upper layers. (**g**) The regions (boxes in right panel) chosen for quantification in sagittal and coronal sections of mouse E17.5 brain are indicated, as well as the plane of sectioning used for quantification. (**h**) Quantification of the proportion of neurons of a certain layer in the total number of cells present in the cortical plate. # $P = 0.006$, ## $P = 0.00057$, ### $P = 0.000051$, * $P = 0.00014$, ** $P = 0.000057$, *** $P = 0.000063$. Error bars indicate s.e.m. Scale bars represent 50 μm.

conclude that the premature generation of layer 2–5 neurons must be a result of a direct effect on cell-fate choice.

## Sip1 controls the timing of glial precursor specification

The results of our BrdU pulse-labeling experiments suggest that neurogenesis in the *Sip1* mutant neocortex ends prematurely at around E15.5 (**Fig. 3a** and data not shown). We wondered whether the neurogenic progenitor pool becomes exhausted at this stage and whether this would influence the subsequent generation of glial cells. Although the overall levels of proliferation at E15.5 and E16.5 were similar in control and mutant cortices, there were much fewer Tbr2-expressing subventricular zone (SVZ) progenitors in the latter (**Supplementary Fig. 3**), further corroborating our claim of a premature end of neurogenesis. Several independent studies have so far failed to establish the ability of Tbr2-positive cells to generate glia; thus, Tbr2 is an indicator of neuronal commitment[21,22]. Because gliogenesis in the mouse neocortex starts at E17.5, we documented cell proliferation at this stage by Ki67 immunostaining. We made two observations. First, the number of dividing cells was significantly higher in mutant brains than in controls ($P = 0.0063$; **Fig. 4a–d**). Second, in contrast with the controls, fewer Ki67-positive cells were found in the ventricular zone/SVZ and significantly more ($P = 0.005$ and $P = 0.0019$; **Supplementary Fig. 3**) were localized to the SVZ/intermediate zone in mutants. This nonventricular mode of cell proliferation is very typical of gliogenic cells at later stages of cortical development. Notably, most of these cells expressed the radial glial marker BLBP, which is characteristic of precursors committed toward an astrocytic lineage (**Supplementary Fig. 3**)[23,24].

To verify this apparent precocious gliogenesis, we traced the fate of dividing cells at E15.5, 16.5 and 17.5 using BrdU pulse chase. We identified glial cells by immunostaining for the markers GFAP (mature astrocytes) and/or Olig2 (glial precursors) (**Fig. 4e–n**). At E16.5, about 45% more Olig2-positive cells were generated in mutant than in control embryos (**Fig. 4h,j,l,n**). We also detected more cells born at E16.5 that differentiated into GFAP-positive astrocytes at P2 and P4 in the mutant neocortex (**Fig. 4g,i,k**). Likewise, most of the cells that incorporated BrdU at E17.5 expressed GFAP or Olig2 at early postnatal stages. Furthermore, we detected about twice as many Olig2-positive cells in the *Sip1|Nestin* neocortex at E18.5 than in the control (data not shown). We also found that glial cells were present in excessive numbers at P2–8 in the mutant neocortex (**Fig. 4e,f,m**). It seems, therefore, that the premature end of neurogenesis paves the way for enhanced proliferation of glial precursors, which in turn leads to the production of higher numbers of astrocytes at early postnatal stages.

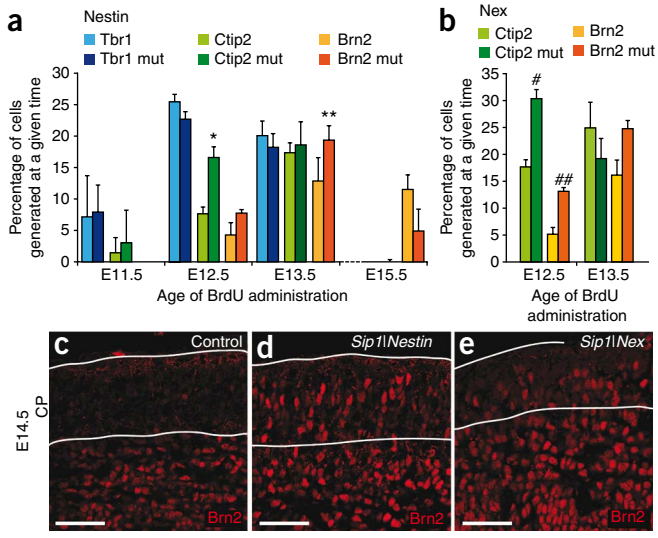


**Figure 3** *Sip1* deletion in neocortical postmitotic cells causes premature generation of layer 2–5 neurons. (**a**) Pulse-chase experiments with BrdU administered at different time points during development (shown on the *x* axis) followed by analysis of the indicated layer-specific markers at E18.5. Quantification of percentages of cells that were stained for both BrdU and the layer-specific marker at the time of analysis, corresponding to different time points of BrdU administration in control and *Sip1|Nestin* (mut) mice. We found no difference in the timing of production of Tbr1-positive neurons. A higher proportion of Ctip2-expressing neurons incorporated BrdU label at E12.5 (* $P = 0.002$) and more Brn2-positive cells were generated at E13.5 (** $P = 0.036$) in the mutant neocortex. At E15.5, no layer 5 and 6 neurons were born in either the control or mutant, whereas the generation of layer 2–4 neurons was nearly complete in the latter. Error bars indicate s.e.m. (**b**) Similar pulse-chase experiments at E12.5 and E13.5 in *Sip1|Nex* and control mice showed increased generation of layer 2–5 neurons (# $P = 0.0047$ and ## $P = 0.013$) at E12.5. Error bars indicate s.e.m. (**c**–**e**) Immunostaining for upper-layer marker Brn2 at E14.5 revealed neurons with upper-layer characteristics in the mutant (*Sip1|Nestin* and *Sip1|Nex*) cortical plate at a stage when such neurons were absent in the control. Scale bars represent 50 μm.

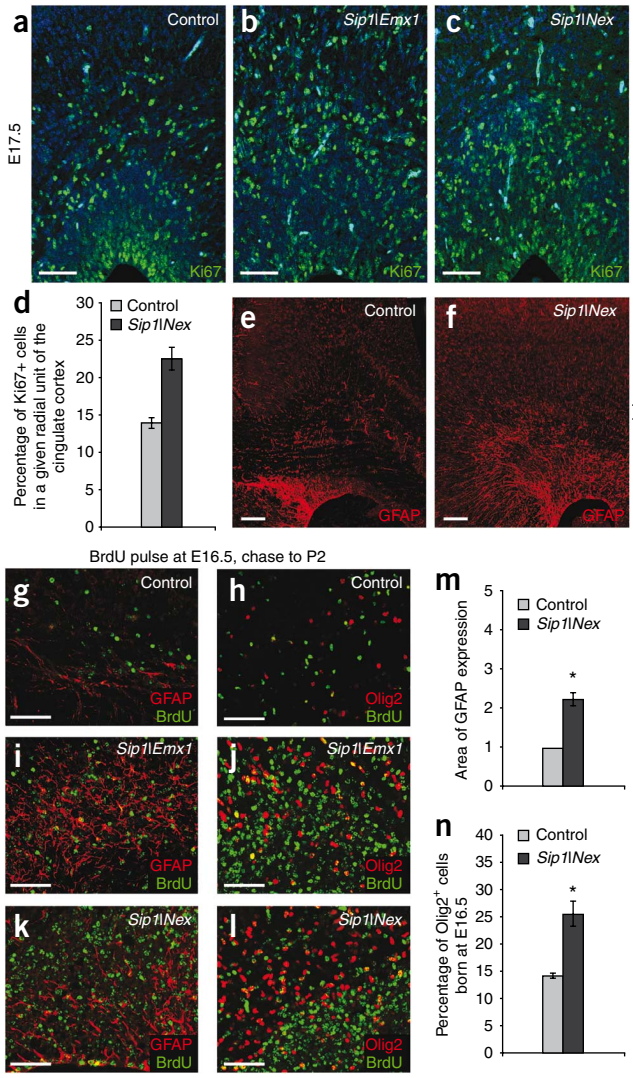


**Figure 4** Enhanced astrocytic proliferation and premature and increased gliogenesis in *Sip1* conditional mutants. (**a**–**c**) Shown here is the expression of proliferation marker Ki67 at E17.5 in control (**a**), *Sip1*|*Emx1* (**b**) and *Sip1*|*Nex* (**c**) mice in a region close to the medial neocortex. (**d**) The increase in proliferation in the mutant neocortex was quantified over an entire radial unit and is represented as the percentage of the total number of cells counted in this unit that were labeled for Ki67. * $P = 0.0063$. (**e**,**f**) Expression of astrocytic marker GFAP was found to be twofold higher in the cingulate neocortex in *Sip1*|*Nex* at P2 (immunostaining for GFAP at P4 shown in **e** and **f**; quantification in **m**). (**g**–**l**) To trace the origin of these astrocytes, we pulse-labeled dividing cells in the neocortex with BrdU at E16.5 and chased them at P2. Double immunostaining for BrdU and GFAP (**g**,**i**,**k**) and for BrdU and Olig2 (**h**,**j**,**l**) indicated that precocious production of glial cells was occurring in *Sip1*|*Emx1* (**i**,**j**) and *Sip1*|*Nex* (**k**,**l**) conditional knockout mice. Scale bars are 50 μm. (**m**) We measured the area of GFAP expression in a specific region of the neocortex in both control and mutant and normalized the mutant values with regard to the control. * $P = 0.0018$. Error bars indicate s.e.m. (**n**) Twice as many Olig2-expressing glial progenitors were born at E16.5 in *Sip1*|*Nex* brains as in control. * $P = 0.0077$. Error bars indicate s.e.m.



## Sip1 restricts *Ntf3* and *Fgf9* expression in neurons

Both the premature switch in cell fate and the excessive production of later-born neocortical cell types are phenotypes that possibly originate from an inappropriate regulation of cell type commitment, which is believed to be determined in precursor cells. Because deletion of *Sip1* in postmitotic cells alone is sufficient to alter progenitor fate, we hypothesized that Sip1 controls the level of expression of growth factors in young neurons. Such factors could then signal back to the progenitors to control both cell-fate switch and the numbers of each cell type produced in the neocortex. To identify these factors, we performed microarray-based gene expression profiling at two time points, E14.5, corresponding to precocious upper layer production, using cortical tissue of *Sip1*|*Nex* and control littermate embryos; and E18.5, corresponding to premature gliogenesis, using *Sip1*|*Nestin* and control littermate tissue.

Sip1 preferentially acts as a transcriptional repressor. We validated the expression levels of genes that had increased expression in mutant tissues using quantitative real-time PCR and *in situ* hybridization (ISH). *Ntf3* and *Fgf9* transcripts were strongly overexpressed in the mutant brains at E14.5 and 16.5, respectively (**Fig. 5a–f**). Expression of *Ntf3* mRNA was detected in Sip1-deficient cortical plate as early as E12.5. At E13.5, 14.5 and 15.5, *Ntf3* mRNA was markedly upregulated as more postmitotic cells began to populate the cortical plate (**Fig. 5a–c** and **Supplementary Fig. 4**). In control embryos, *Ntf3* mRNA levels remained low at these stages and only increased locally at late gestation (E17.5) (**Fig. 5a**, **Supplementary Fig. 4** and data not shown). Increased *Fgf9* mRNA levels were detected prematurely at E16.5 in the mutant neocortex. As with *Ntf3*, *Fgf9* expression was also upregulated in the mutant cortical plate cells, in contrast with control embryos, in which it remained low, including at later stages (**Fig. 5d–f** and **Supplementary Fig. 4**).

We then tested *Ntf3* and *Fgf9* as possible direct target genes of Sip1. We carried out chromatin immunoprecipitation (ChIP) with antibody to Sip1 on chromatin isolated from cortical tissue at E16.5–17.5. Sip1 interacts with regulatory elements containing a tandem of two sequences (CAC CT(G) and/or, in fewer cases, CAC ANN T) separated by a varying number of base pairs[25]. We designed several primer pairs within 5,000-bp upstream of the first exon of *Ntf3* and *Fgf9* and analyzed the immunoprecipitate via qualitative PCR. We found a significantly higher ($P = 0.044$) level of interaction of Sip1 with the −1,300 region of *Ntf3* (**Fig. 5g**), but we could not detect any preferential binding of Sip1 with the *Fgf9* upstream region. We also tested three intronic regions of *Fgf9* that contain putative Sip1 binding sites, but none of these were preferentially bound by Sip1 (**Fig. 5g** and data not shown). Therefore, Sip1 seems to interact directly with the promoter region of mouse *Ntf3*, possibly repressing its transcription. On the other hand, although *Fgf9* expression was clearly regulated by Sip1, it remains unclear as to whether this is mediated via direct physical interaction.

If Ntf3 and Fgf9 act as feedback signaling factors from the cortical plate to the progenitor cells, their cognate receptors should be present on ventricular zone cells. Ntf3 has been shown to bind to TrkC, whereas Fgf9 binds to Fgfr2 and Fgfr3 (refs. 26,27). We analyzed the expression of these receptors by ISH at E14.5 (for *TrkC*) and 16.5 (for *Fgfr2* and *Fgfr3*) and found no differences between control and mutant neocortex (**Fig. 5h–m**). Both TrkC and Fgfr3 were found in progenitors and would thus be the candidate receptors for transducing Ntf3 and Fgf9 signals, respectively.

## Addition of Fgf9 to cortical slices enhances gliogenesis

Precocious expression of *Ntf3* in *Sip1* mutant brains at E12.5 coincides with premature production of upper-layer cells, whereas precocious upregulation of *Fgf9* coincides with premature specification of glial precursors. To determine whether these factors alone can

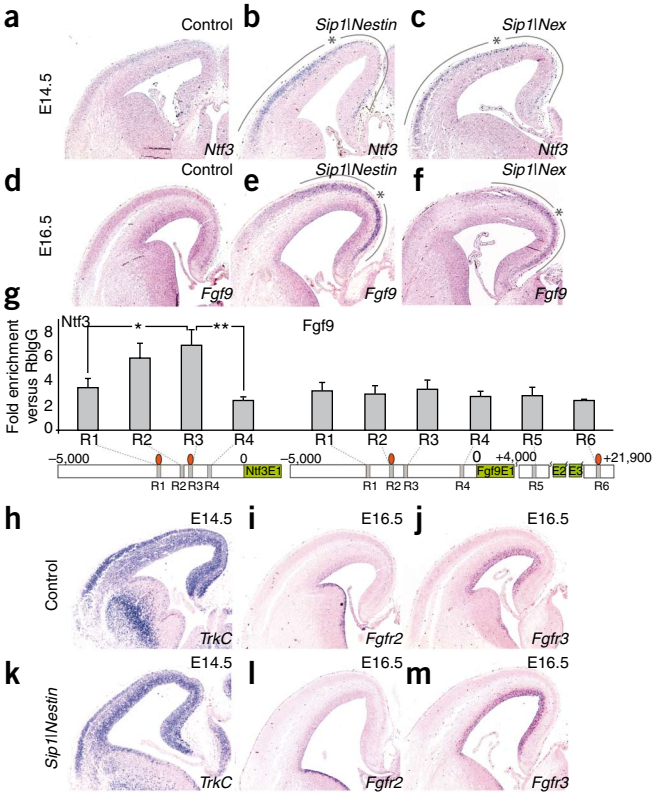


**Figure 5** *Ntf3* and *Fgf9* steady-state mRNA levels are upregulated in the embryonic neocortex in the absence of Sip1. (**a**–**f**) ISH of *Ntf3* (**a**–**c**) and *Fgf9* (**d**–**f**) mRNA at E14.5 and 16.5 respectively, showed upregulation of both in the Sip1-deficient cortical plate. *Fgf9* was found more in the cingulate cortex, whereas *Ntf3* was detected in the entire cortical plate (line with star). (**g**) Different regions (R) within 5-kb upstream of the first exon of the *Ntf3* and *Fgf9* genes were tested for interaction with Sip1 by ChIP. The graph shows the relative enrichment of these regions for rabbit antibody to Sip1–immunoprecipitated DNA versus rabbit IgG–immunoprecipitated DNA. In the sketch, gray rectangles depict the regions that were amplified by validated primer sets. Putative tandem Sip1-binding sites are represented by red ellipses. Only R3 seems to be bound by Sip1 (* $P = 0.047$ and ** $P = 0.044$, error bars indicate s.e.m.). In the *Fgf9* regulatory region, we could not detect specific interaction with four regions in the upstream regulatory region and two regions in intronic sequences. (**h**,**k**) ISH for the Ntf3 receptor *TrkC* at E14.5 showed high mRNA expression levels in the entire neocortex. (**i**,**l**) ISH for the Fgf9 receptor *Fgfr2* showed expression localized to the ventricular zone of the ganglionic eminences at E16.5. (**j**,**m**) *Fgfr3* at E16.5 were highly expressed in the neocortical ventricular zone.

mimic the *Sip1* mutant phenotype *in vitro*, we added them to organotypic cultures of wild-type cortical tissue.

At first, we cultured E12.5 and 13.5 wild-type cortical explants with or without Ntf3. After 2–3 d, we estimated the ratio of Satb2- to Ctip2- or Sox5-positive cells in these explants. The addition of Ntf3 (up to 600 ng ml$^{-1}$) did not cause an increase in these ratios compared to nontreated explants. To determine whether Fgf9 can influence cortical gliogenesis, we cultured cortical slices prepared from E16.5 wild-type brains in the presence of varying concentrations of Fgf9. After 2 d, we analyzed the numbers of Olig2-expressing cells in the neocortex. The slices treated with Fgf9 (20 ng ml$^{-1}$) were found to contain 2.7-fold more Olig2-positive cells than the control (**Fig. 6a–d**). Notably, most of these cells were localized close to the ventricle, although Fgf9 was present homogenously throughout the culture medium. These experiments indicate that Fgf9, when added to organotypic cultures, can mimic the enhanced gliogenesis observed in the *Sip1* mutant neocortex. To determine whether this

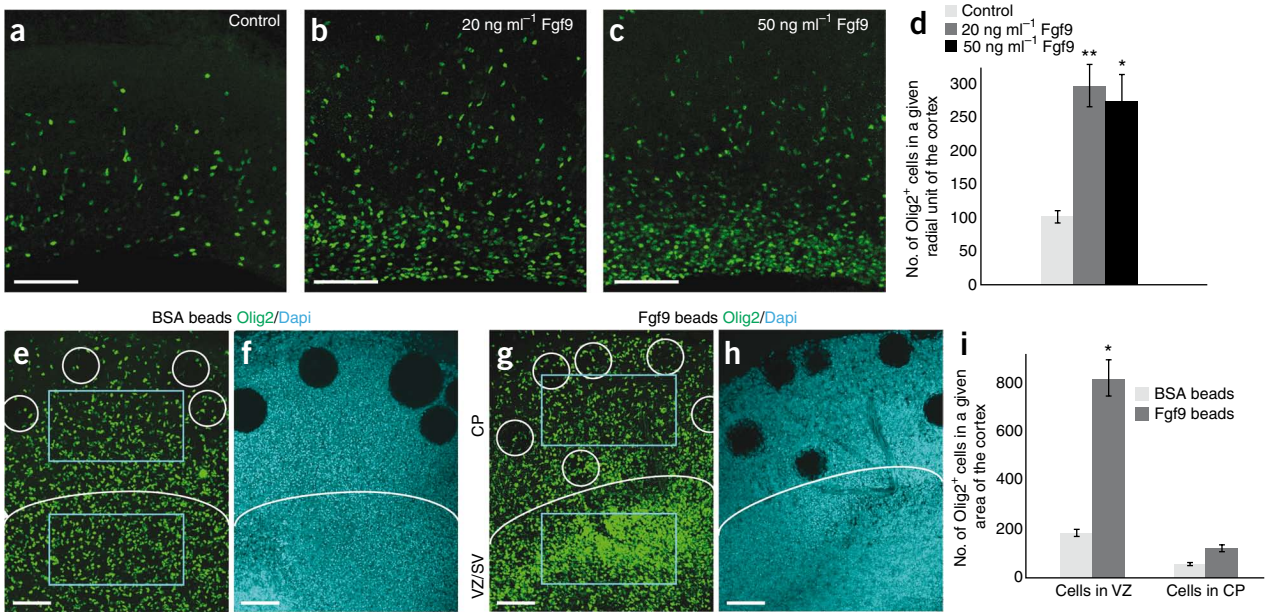


**Figure 6** Fgf9 can induce increased production of Olig2-expressing glial progenitors in wild-type forebrain slices *in vitro*. (**a**–**d**) E16.5 wild-type slices treated with different concentrations of soluble Fgf9 and cultured for 2 d *in vitro* were stained for Olig2. Control slices and slices treated with 20 and 50 ng ml$^{-1}$ Fgf9 are shown. There were 2.7-fold more Olig2-positive cells in Fgf9-treated slices (**d**) than in control slices. ** $P = 0.0001$, * $P = 0.01$. Error bars indicate s.e.m. (**e**–**i**) Localized (through beads) application of Fgf9 in the cortical plate (CP) also induced gliogenic proliferation specifically in the ventricular zone (VZ). Fgf9-coated (**g**,**h**) and BSA-coated (**e**,**f**) beads were placed in the cortical plate of E17.5 wild-type slices and cultured for 2 d *in vitro*. Olig2 (**e**,**g**) and nuclei (using DAPI; **f**,**h**) staining is shown. White circles indicate the position of the beads, as can also be seen in the DAPI-stained image. The increase in the number of Olig2-positive cells under the two different conditions is quantified in defined regions (indicated by blue rectangles) of either the cortical plate or the ventricular zone/SVZ. (**i**). Error bars indicate s.e.m. Scale bars represent 100 μm.

effect of Fgf9 originates in the cortical plate and is directed toward the ventricular zone/SVZ, thereby resembling a feedback signaling mechanism, we carried out a second set of *in vitro* experiments. We placed Fgf9-coated agarose beads at precise locations in the cortical plate of E16.5 or 17.5 wild-type slices, thereby ensuring localized application of Fgf9 only in the postmitotic compartment and not in the germinal zones. As a control, we used BSA-coated beads. After 2 d in culture, we quantified the number of Olig2-expressing cells in two different regions of the neocortex, in the ventricular zone/SVZ and in the cortical plate (**Fig. 6e–h**). We detected a ~4.5-fold increase in the number of Olig2-positive glial precursors in the ventricular zone/SVZ of slices implanted with Fgf9-coated beads, whereas BSA-coated beads did not seem to have any effect on the Olig2 domain. There was also a smaller increase in the number of Olig2-positive cells in the cortical plate with Fgf9-coated beads (**Fig. 6i**). Therefore, it seems that a source of Fgf9 in the cortical plate can induce an expansion of the glial precursor pool in the ventricular zone/SVZ, corroborating our claim of a Sip1-controlled feedback signal.

### Precocious MAPK signaling in Sip1 mutant progenitors

Sip1 controls the level of expression of *Ntf3* in young neocortical neurons. Also, as Sip1 seems to influence progenitor fate non–cell autonomously, we suspected that Ntf3 signals back to ventricular zone progenitor cells and elicits an appropriate molecular response. Because we were unable to determine its effect on fate specification *in vitro*, we decided to investigate the activation of downstream signaling pathways *in vivo*. Neurotrophins have been shown to induce cell differentiation through MAPK activation[28]. We immunostained control and mutant cortices for phospho-MAPK p42/44 and phospho-MAPK p38 (**Supplementary Fig. 5**). In addition, we checked activation of downstream effectors of other pathways: phosphorylated forms of CREB, Akt, JNK and phospholipase Cγ (**Supplementary Fig. 5** and data not shown). Of these, only phosphorylated MAPK p42/44 was clearly detected in neocortical progenitors. At E14.5, we found high levels of phospho-MAPK p42/44 in cells of the lateral ventricular zone and low levels in the medial ventricular zone of control neocortex. In the mutant, this staining was much stronger in the ventricular zone throughout the neocortex (**Supplementary Fig. 5**). MAPK activation in the ventricular zone/SVZ reached a maximum at E14.5 in the mutant neocortex (in contrast with E15.5 in control), indicating that progenitor cells must have sensed and, consequently, responded to the increased Ntf3 signal from the cortical plate.

These data indicate that the absence of Sip1 in young neurons induces a premature peak of MAPK signaling in the progenitors. Our findings indicate that Sip1 functions in the postmitotic compartment of the neocortex to control the expression of growth factor genes and thus influence the level of their signaling activity in progenitor cells.

## DISCUSSION

We found that the temporal sequence of progenitor cell fate switch and the numbers of different cell types produced in the neocortex are controlled extrinsically during corticogenesis. Furthermore, we found that the transcription factor Sip1, which is highly expressed in postmitotic neurons throughout neocortical development, seems to regulate the production of signals from postmitotic cells back to the germinal zone to ensure sequential generation of appropriate numbers of different neuronal cell types and glia.

The ability of neuronal progenitor cells to produce different cell types at different developmental stages has been proposed as an intrinsic capacity of the progenitors and was initially based on studies in neuroblasts of *Drosophila*[29]. There are many indications that cortical progenitors are also intrinsically programmed to produce sequential cohorts of different cells[2,8,30]. Isolated cortical progenitors can recapitulate *in vitro* the authentic sequence of generation of these cell types[6,8]. An internal clock-like mechanism capable of counting the number of cell divisions that a progenitor cell goes through has also been proposed. Recently, it was shown that embryonic stem cells can be driven toward cells with dorsal telencephalic fate by blocking Shh-mediated signaling[30,31]. However, the amount of upper-layer neurons generated in these cultures was lower, suggesting that extrinsic factors that influence upper-layer cell fate were present. Other reports have also suggested that extrinsic signals are needed for cell-fate specification. Neurons can, for example, signal back to progenitor cells via cardiotrophin-1 and, in doing so, instruct them to produce astrocytes instead of neurons[9]. Brain-derived neurotrophic factor (BDNF) administered in the ventricular lumen at E13.5 induces deep-layer characteristics in cells destined for layer 4, whereas an antibody to BDNF changed some of these cells to layer 2/3 type neurons, suggesting that BDNF is an extrinsic cortical cell-fate modifier[32].

In other systems, the regulation of neurogenesis is not completely reliant on the intrinsically programmed progenitors either. For instance, in the mammalian eye, a feedback signaling mechanism ensures normal production of different retinal cell types. Similar to the neocortex, these are also produced in sequential, but overlapping, phases. On one hand, late-born rod cell progenitors, when cocultured with early retinal cells, generate far fewer rod cells, possibly as a result of activation of CNTF/LIF signaling[33,34]. On the other hand, young retinal progenitors, when cocultured with older cells, lose the ability to generate early-born amacrine and ganglion cells. It seems that differentiated amacrine and ganglion cells secrete an inhibitory feedback signal that acts at around the last mitotic division to inhibit specification of early-born cell fates[33,35]. Hence, differentiated retinal cells can restrict the fate of embryonic progenitors by relaying feedback information[33,36,37]. Our description of Sip1-mediated signaling is, to the best of our knowledge, the first evidence supporting such a mechanism in the neocortex.

Although *Sip1* mRNA levels were high in the cortical plate, they were very low to nearly undetectable in the ventricular zone/SVZ, and we were never able to detect Sip1 protein in these cells. Together with the *Sip1|Nex* phenotype, this indicates that Sip1 functions in young postmitotic neurons to target progenitor cells in the embryonic neocortex. This effect would most likely be transmitted via secreted factors and interpreted by their cognate receptors on ventricular zone/SVZ progenitors, with the eventual outcome of regulating cell numbers. This concept is akin to that of 'chalones', negative feedback factors secreted by tissues in proportion to their size to inhibit their own growth and eventually stabilize the size of the organ[38–40].

Nothing is known about how cortical progenitor cells learn how many cells of every type should be produced and when the switch from producing one cell type to another has to operate. One method for such control would be a feedback mechanism, in which postmitotic cells would express and secrete very low to low levels of certain factors. These factors would not be sensed by the progenitor cells at low concentrations. However, as neocorticogenesis proceeds and the number of postmitotic cells grows, the concentration of such factors would also increase and, on reaching a certain threshold, would be sensed by progenitors. This would in turn inhibit the generation of an earlier cell type and/or stimulate the generation of the next (**Supplementary Fig. 6**). If such factors exist, their expression levels would ideally be under extremely tight control, as an elevated expression would lead to a change in the cellular composition of the neocortex. The neocortical phenotype in *Sip1* mutants fits very well

with this model. Indeed, the removal of Sip1 from postmitotic cells results in inappropriate numbers of most cell types of the neocortex and their premature production. This model predicts that factors that act downstream of the transcriptional repressor Sip1 should be upregulated exclusively in the cortical plate of *Sip1* mutant neocortex. We identified two such factor-encoding genes, *Ntf3* and *Fgf9*, which are expressed by cortical plate cells in the wild-type neocortex at lower levels because of Sip1-mediated repression.

The premature onset of *Ntf3* expression in *Sip1* mutant neocortex at E12.5 and of *Fgf9* at E16.5 precedes the precocious cell fate change from deep- to upper-layer neurons at E12.5–13.5 and coincides with a switch from production of neurons to glial cells at E16.5–17.5. Although the precise location of Fgf receptors on ventricular zone progenitors is not known, there are two possible mechanisms by which Fgf9 could signal to the latter. On one hand, Fgf receptors could be distributed on radial glial processes, so that Fgf9 secreted by cortical plate neurons would find its binding partner almost immediately and the intracellular signaling cascade would travel down the processes to the ventricular zone. On the other hand, Fgf9 could physically diffuse, as in the *in vitro* slices, into the ventricular zone, bind to receptors and elicit the appropriate response. In either case, it is clear that Fgf9 acts in a paracrine fashion. Fgf9 has been shown to induce cell-fate switch and promote gliogenesis in other systems as well. When it is ectopically expressed in retinal pigment epithelium, these cells lose their retinal pigment epithelium character, undergo a cell-fate switch and become neural retina[41]. Also, exogenous application of Fgf9 induces proliferation of Fgfr2/3-positive Müller glial cells *in vitro*[42]. In the neocortex, analysis of both *Fgfr2* and *Gfap* conditional knockouts and *Fgfr1/Fgfr2* and *Gfap* double mutants showed a decrease in the density of astrocytes in the dorsal neocortex[43].

A previous study[44] found that cultured neocortical progenitor cells respond to a stimulus of Ntf3 by activating MAPK-ERK, which results in cell differentiation. More recent *in vivo* work showed that blocking Ntf3 signaling in neocortical progenitors results in increased cell numbers in deep layers, which is consistent with a failure of the progenitors to switch to the production of the next neocortical layer[45]. We found that MAPK activity in ventricular zone cells is indeed affected in *Sip1* mutants. MAPK activation peaks in wild-type cortical ventricular zone precursors at E15.5 and in mutant neocortex at E14.5, coinciding with the time of generation of most upper-layer neurons. Notably, a lateral-to-medial gradient of MAPK activity in ventricular zone progenitors is identical to the lateral-to-medial gradient of neocortical maturation. Upper-layer production is a part of this maturation. This strongly indicates that extrinsic signaling controlled by Sip1 causes cell-fate switch in progenitors. Whether Ntf3 itself is the only factor causing this shift remains to be studied. Also to be determined are the other signaling proteins that presumably act in concert with Ntf3 to influence early neocortical progenitor fate.

In summary, our work provides, to the best of our knowledge, the first evidence of neuron-to-progenitor feedback signaling in the neocortex regulating the fate of uncommitted precursors and ensuring production of appropriate numbers of different neurons and glia. Our results establish Sip1 as an important mediator of this mechanism through its negative regulation of expression of secreted factors in postmitotic neurons.

## METHODS

Methods and any associated references are available in the online version of the paper at http://www.nature.com/natureneuroscience/.

**Accession numbers.** The data obtained in our microarray experiments were deposited at the GEO website under accession number GSE16699.

*Note: Supplementary information is available on the Nature Neuroscience website.*


## ACKNOWLEDGMENTS

We thank the Flanders Institute for Biotechnology Microarray Facility, J. Allemeersch and P. Van Hummelen for their skillful analysis of our samples. We thank R. Hevner, D. Ornitz, L. Lei, J. Alberta and C. Stiles for reagents; P. Vanderhaeghen for advice and G. Fishell for numerous discussions. The D.H. laboratory thanks H. Van den Berghe for continuous support. E.S. was a postdoctoral fellow with the Research Foundation Flanders and the Franqui Foundation. This study was supported by the Research Foundation Flanders (G.0288.07), the inter-universitary attraction pole network (IUAP-PAI 6/20) and the EC-FP6 Project Endotrack (LSHG-CT-2006-19050). The V.T. laboratory was supported by Max-Planck Society, Heisenberg Program and Exc 257 of Deutsche Forschungsgemeinschaft, and Fritz Thyssen Foundation. A.N. was a Marie Curie Host Fellow For Early Stage Researchers Training (NEUREST MEST-CT-2004-504193).


## AUTHOR CONTRIBUTIONS

E.S., A.N., A.M., D.H. and V.T. designed the experiments, E.S., A.N., A.M., J.D. and A.S. conducted the experiments, and S.G and K.-A.N. provided *Nex-cre* mice. V.T. wrote the manuscript and E.S., A.N. and D.H. edited the manuscript.

Published online at http://www.nature.com/natureneuroscience/.
Reprints and permissions information is available online at http://www.nature.com/reprintsandpermissions/.




1. Williams, B.P. & Price, J. Evidence for multiple precursor cell types in the embryonic rat cerebral cortex. *Neuron* **14**, 1181–1188 (1995).
2. Temple, S. The development of neural stem cells. *Nature* **414**, 112–117 (2001).
3. Desai, A.R. & McConnell, S. Progressive restriction in fate potential by neural progenitors during cerebral cortical development. *Development* **127**, 2863–2872 (2000).
4. Morrow, T., Song, M.-R. & Ghosh, A. Sequential specification of neurons and glia by developmentally regulated extracellular factors. *Development* **128**, 3585–3594 (2001).
5. Bayer, S.A. & Altman, J. *Neocortical Development* (Raven Press, New York, 1991).
6. Qian, X. *et al.* Timing of CNS cell generation: a programmed sequence of neuron and glial cell production from isolated murine cortical stem cells. *Neuron* **28**, 69–80 (2000).
7. McConnell, S.K. Fates of visual cortical neurons in the ferret after isochronic and heterochronic transplantation. *J. Neurosci.* **8**, 945–974 (1988).
8. Shen, Q. *et al.* The timing of cortical neurogenesis is encoded within lineages of individual progenitor cells. *Nat. Neurosci.* **9**, 743–751 (2006).
9. Barnabé-Heider, F. *et al.* Evidence that embryonic neurons regulate the onset of cortical gliogenesis via cardiotrophin-1. *Neuron* **48**, 253–265 (2005).
10. Verschueren, K. *et al.* SIP1, a novel zinc finger/homeodomain repressor, interacts with Smad proteins and binds to 5′-CACCT sequences in candidate target genes. *J. Biol. Chem.* **274**, 20489–20498 (1999).
11. Verstappen, G. *et al.* Atypical Mowat-Wilson patient confirms the importance of the novel association between ZFHX1B/SIP1 and NuRD corepressor complex. *Hum. Mol. Genet.* **17**, 1175–1183 (2008).
12. van Grunsven, L.A. *et al.* Delta-EF1 and SIP1 are differentially expressed and have overlapping activities during *Xenopus* embryogenesis. *Dev. Dyn.* **235**, 1491–1500 (2006).
13. Dastot-Le Moal, F. *et al.* ZFHX1B mutations in patients with Mowat-Wilson syndrome. *Hum. Mutat.* **28**, 313–321 (2007).
14. Van de Putte, T. *et al.* Mice lacking ZFHX1B, the gene that codes for Smad-interacting protein- 1, reveal a role for multiple neural crest cell defects in the etiology of Hirschsprung disease-mental retardation syndrome. *Am. J. Hum. Genet.* **72**, 465–470 (2003).
15. Tronche, F. *et al.* Disruption of the glucocorticoid receptor gene in the nervous system results in reduced anxiety. *Nat. Genet.* **23**, 99–103 (1999).
16. Goebbels, S. *et al.* Genetic targeting of principal neurons in neocortex and hippocampus of *Nex-cre* mice. *Genesis* **44**, 611–621 (2006).
17. Gorski, J.A. *et al.* Cortical excitatory neurons and glia, but not GABAergic neurons, are produced in the Emx1-expressing lineage. *J. Neurosci.* **22**, 6309–6314 (2002).
18. Miquelajauregui, A. *et al.* Smad-interacting protein-1 (Zfhx1b) acts upstream of Wnt signaling in the mouse hippocampus and controls its formation. *Proc. Natl. Acad. Sci. USA* **104**, 12919–12924 (2007).
19. Higashi, Y. *et al.* Generation of the floxed allele of the *SIP1* (*Smad-interacting protein 1*) gene for Cre-mediated conditional knockout in the mouse. *Genesis* **32**, 82–84 (2002).
20. Wu, S.-X. *et al.* Pyramidal neurons of upper cortical layers generated by NEX-positive progenitor cells in the subventricular zone. *Proc. Natl. Acad. Sci. USA* **102**, 17172–17177 (2005).
21. Noctor, S.C., Martinez-Cerdeno, V., Ivic, L. & Kriegstein, A.R. Cortical neurons arise in symmetric and asymmetric division zones and migrate through specific phases. *Nat. Neurosci.* **7**, 136–144 (2004).

22. Arnold, S.J. *et al.* The T-box transcription factor Eomes/Tbr2 regulates neurogenesis in the cortical subventricular zone. *Genes Dev.* **22**, 2479–2484 (2008).
23. Hartfuss, E., Galli, R., Heins, N. & Götz, M. Characterization of CNS precursor subtypes and radial glia. *Dev. Biol.* **229**, 15–30 (2001).
24. Nieto, M., Schuurmans, C., Britz, O. & Guillemot, F. Neural bHLH genes control the neuronal versus glial fate decision in cortical progenitors. *Neuron* **29**, 401–413 (2001).
25. Remacle, J.E. *et al.* New mode of DNA binding of multi-zinc finger transcription factors: deltaEF1 family members bind with two hands to two target sites. *EMBO J.* **18**, 5073–5084 (1999).
26. Huang, E.J. & Reichardt, L.F. Trk receptors: roles in neuronal signaling. *Annu. Rev. Biochem.* **72**, 609–642 (2003).
27. Eswarakumar, V.P., Lax, I. & Schlessinger, J. Cellular signaling by fibroblast growth factor receptors. *Cytokine Growth Factor Rev.* **16**, 139–149 (2005).
28. Kaplan, D.R. & Miller, F.D. Neurotrophin signal transduction in the nervous system. *Curr. Opin. Neurobiol.* **10**, 381–391 (2000).
29. Grosskortenhaus, R., Pearson, B.J., Marusich, A. & Doe, C.Q. Regulation of temporal identity transitions in *Drosophila* neuroblasts. *Dev. Cell* **8**, 193–202 (2005).
30. Gaspard, N. *et al.* An intrinsic mechanism of corticogenesis from embryonic stem cells. *Nature* **455**, 351–357 (2008).
31. Eiraku, M. *et al.* Self-organized formation of polarized cortical tissues from ESCs and its active manipulation by extrinsic signals. *Cell Stem Cell* **3**, 519–532 (2008).
32. Fukumitsu, H. *et al.* Brain-derived neurotrophic factor participates in determination of neuronal laminar fate in the developing mouse cerebral cortex. *J. Neurosci.* **26**, 13218–13230 (2006).
33. Belliveau, M.J. & Cepko, C. Extrinsic and intrinsic factors control the genesis of amacrine and cone cells in the rat retina. *Development* **126**, 555–566 (1999).
34. Neophytou, C., Vernallis, A., Smith, A. & Raff, M. Muller cell–derived leukaemia inhibitory factor arrests rod photoreceptor differentiation at a postmitotic pre-rod stage of development. *Development* **124**, 2345–2354 (1997).
35. Zhang, X.M. & Yang, X. Regulation of retinal ganglion cell production by Sonic hedgehog. *Development* **128**, 943–957 (2001).
36. Waid, D.K. & McLoon, S. Ganglion cells influence the fate of dividing retinal cells in culture. *Development* **125**, 1059–1066 (1998).
37. Pearson, B.J. & Doe, C.Q. Specification of temporal identity in the developing nervous system. *Annu. Rev. Cell Dev. Biol.* **20**, 619–647 (2004).
38. Bullough, W.S. L.E. Mitotic control by internal secretion: the role of the chalone-adrenalin complex. *Exp. Cell Res.* **33**, 176–194 (1964).
39. Lee, S.-J. & McPherron, A.C. Myostatin and the control of skeletal muscle mass. *Curr. Opin. Genet. Dev.* Commentary **9**, 604–607 (1999).
40. Lander, A.D.G.K., Wan, F.Y., Nie, Q. & Calof, A.L. Cell lineages and the logic of proliferative control. *PLoS Biol.* **7**, e15 (2009).
41. Zhao, S. *et al.* Patterning the optic neuroepithelium by FGF signaling and Ras activation. *Development* **128**, 5051–5060 (2001).
42. Cinaroglu, A.O.Y., Ozdemir, A., Ozcan, F., Ergorul, C., Cayirlioglu, P., Hicks, D. & Bugra, K. Expression and possible function of fibroblast growth factor 9 (FGF9) and its cognate receptors FGFR2 and FGFR3 in postnatal and adult retina. *J. Neurosci. Res.* **79**, 329–339 (2005).
43. Smith, K.M. *et al.* Midline radial glia translocation and corpus callosum formation require FGF signaling. *Nat. Neurosci.* **9**, 787–797 (2006).
44. Barnabé-Heider, F. & Miller, F.D. Endogenously produced neurotrophins regulate survival and differentiation of cortical progenitors via distinct signaling pathways. *J. Neurosci.* **23**, 5149–5160 (2003).
45. Bartkowska, K., Paquin, A., Gauthier, A.S., Kaplan, D.R. & Miller, F.D. Trk signaling regulates neural precursor cell proliferation and differentiation during cortical development. *Development* **134**, 4369–4380 (2007).

## ONLINE METHODS

**Mouse mutants and BrdU injection.** All mouse experiments were carried out in compliance with Belgian and German law and according to the guidelines of the Animal Care Committee of Katholieke Universiteit Leuven or were approved by the Bezirksregierung Braunschweig. Mice carrying *loxP*-flanked (exon7) *Sip1* alleles ($Sip1^{loxP/loxP}$) were crossed with various Cre lines that were heterozygous for *Sip1* or $Sip1^{loxP/+}$ to generate *cre;* $Sip1^{loxP/-}$ or *cre;* $Sip1^{loxP/loxP}$ mice (conditional mutants), and *cre;* $Sip1^{loxP/+}$, $Sip1^{loxP/-}$, $Sip1^{loxP/loxP}$ or $Sip1^{loxP/+}$ mice (controls). For birthdating experiments, BrdU (100 mg per kg of body weight) was injected intraperitoneally at various stages and embryos were recovered at E18.5 (for neurogenesis experiments) or at P2–8 (for gliogenesis).

**Immunohistochemistry, microscopy and data analysis.** Brains were dissected and washed in ice-cold phosphate-buffered saline (PBS) and fixed overnight with 4% paraformaldehyde (wt/vol) followed by progressive alcohol-assisted dehydration and paraffin embedding. Frontal 6-μm-thick sections (**Figs. 1–3** and **5**, and **Supplementary Figs. 2, 4** and **5**) were processed for immunohistochemistry using an automated platform (Ventana Discovery, Ventana Medical Systems) and mounted in DAPI-supplemented Mowiol. We used rabbit antibody to Sip1 (1:100, Genscript custom antibody against a GST-fusion peptide containing the N-terminal part of Sip1), rabbit antibody to Tbr1 (from R. Hevner, University of Washington) and Chemicon, 1:3,000), rat antibody to Ctip2 (Abcam, ab18465, 1:300), goat antibody to Brn2 (Santa Cruz, 1:60), rabbit antibody to Satb2 (1:300), monoclonal antibody to BrdU (Roche, 1:300), rabbit antibody to Ki67 (Novocastra, NCL-Ki67p, 1:50), rabbit antibody to phospho-p44/42 MAPK (Cell Signaling Technology, #4370, 1:600), rabbit antibody to phospho-p38 (Cell Signaling Technology, #9198, 1:150) and rabbit antibody to phospho-CREB (Cell Signaling Technology, #4668, 1:300) as primary antibodies. For secondary antibodies, we used CY2-, CY3- or biotin-conjugated donkey antibody to rabbit IgG, CY2-conjugated donkey antibody to rat IgG, CY2- or CY3-conjugated donkey antibody to goat IgG, and CY3-conjugated donkey antibody to mouse IgG (all at 1:600, Jackson ImmunoResearch). Nonfluorescent immunostaining was carried out with DAB. Sections were photographed using a confocal radiance microscope connected to a spot camera (Visitron Systems) and data analysis was done with ImageJ software (US National Institutes of Health). For each experiment, at least three control and three knockout brains were analyzed. For lamination and BrdU pulse-chase experiments, three sections per brain were quantified. In each brain, marker-positive cells in a radial unit of 350 μm were quantified in two regions (one medial and one lateral) in the same coronal plane. For the BrdU experiments, BrdU and marker-positive double-labeled cells were quantified as a percentage of all marker-positive cells. The cells were counted using ImageJ and the data from of all of the regions were pooled. Statistical analysis was done with Excel software (Microsoft).

For **Figures 4** and **6** and **Supplementary Figures 1** and **3**, we cut 10-μm-thick frontal sections on a Leica microtome. For immunostaining, the sections were first rehydrated, followed by antigen unmasking (Vector Laboratories) and pretreatment with HCl (for labeling involving antibody to BrdU). Sections were blocked for 1 h at 24 °C with a solution of 0.1% Tween20 (vol/vol) and 1% BSA (wt/vol) in PBS. We used antibody to BrdU (Abcam, ab6326, 1:100), antibody to GFAP (Cy3-conjugated, Sigma, C-9205, 1:500), antibody to Ki67 (DakoCytomation, M7249, 1:30) and antibody to Olig2 (J. Alberta and C. Stiles, Dana-Farber Cancer Institute, 1:20,000) as primary antibodies and we used Hoechst dye (Sigma, B2261, 1:500). All antibodies were incubated with slides overnight at 4 °C except for the antibody to GFAP, which was incubated for not more than 45 min at 24 °C. Alexa Fluor–tagged secondary antibodies were from Invitrogen (Molecular Probes) and used at a dilution of 1:500. All sections were mounted in fluorescent mounting medium (DakoCytomation, s3023). Images were made on a Leica confocal microscope. For BrdU and GFAP colocalization studies, images were procured at a pinhole of 1 Airy unit (AU), followed by spectral unmixing in the Leica confocal software. Image processing (contrast-enhancement, assembly into montages), analysis and quantification were carried out using Adobe Photoshop and ImageJ, as described previously. To quantify the extent of proliferation at E17.5 in control and *Sip1|Nex* cortices, we chose a radial unit (220 μm width) in the region of the cingulate neocortex and calculated the fraction of Ki67-positive cells in the total number of cells in the unit (based on staining with DAPI) for three control and three mutant brains from three different litters, taking an average of four sections per brain. The cells were counted manually and using ImageJ. To calculate the level of GFAP expression at P2, a region of 293 × 403 μm was chosen close to the ventricle and in the cingulate neocortex. The area of GFAP expression was then measured in this region using ImageJ. The values in mutant cortices were normalized with respect to the area of staining in control cortices. This was done in three control and three *Sip1|Nex* brains from three different litters, taking an average of three to four sections per brain. To determine the extent of glial fate specification at E16.5 in control and *Sip1|Nex* cortices, we selected an entire radial unit of 256 μm width in the cingulate neocortex and determined the absolute number of BrdU-positive, Olig2-positive and double-positive cells manually. We then calculated the fraction of Olig2-positive cells at P2 that were labeled with BrdU. For both control and *Sip1|Nex* cortices, this value was determined as an average of three brains each (an average of four to six sections per brain) from three different litters. To determine the level of neurogenesis in control and *Sip1|Nex* cortices at E16.5 (**Supplementary Fig. 3**), we selected an area of 220 × 256 μm in the ventricular zone/SVZ (from ventricular surface to the intermediate zone). In this region, the numbers of Tbr2-positive cells and the total number of cells (DAPI) were counted using ImageJ. The fraction of the total number of cells at the ventricular zone/SVZ that were Tbr2 positive is represented in the graph shown in **Supplementary Figure 3**. Once again, this fraction was calculated in three control and three *Sip1|Nex* brains.

**Slice culture.** We cut 200–250-μm-thick sections of E16 wild-type brains using a Leica vibratome and cultured them on cell-culture inserts (1-μm pore size, BD Biosciences) according to the protocol described previously[46]. The slice culture medium consisted of complete Hank's Balanced Salt Solution, basal medium Eagle, 20 mM D-glucose, 1 mM L-glutamine, penicillin (100 U $ml^{-1}$), streptomycin (0.1 mg $ml^{-1}$), N2 supplement (100 μl per 12.5 ml) and 10% heat-inactivated horse serum (vol/vol). Slices were treated with 20–50 ng $ml^{-1}$ mouse Fgf9 (Peprotech, 450-30) and cultured for two division rounds. Only one dose was given at approximately 1 h after the slices were plated. After culturing, the slices were fixed in 4% paraformaldehyde for 30 min before immunostaining, which was done according to standard protocols using 0.5% Triton X-100 and 2% BSA in PBS. Primary antibody incubation was carried out overnight at 4 °C. Images were procured on Leica confocal microscope at a pinhole of 1 AU and were processed and analyzed using Adobe Photoshop and ImageJ. For quantification of Olig2-positive cells, we first selected slices at similar levels along the rostrocaudal axis. An entire radial unit (366 μm width) was then chosen in every slice and the number of Olig2-positive cells in this unit was quantified using ImageJ. The data shown in the graph in **Figure 6** was obtained from three independent experiments, using slices from five to eight wild-type brains in each experiment.

**Slice culture with implantation of Fgf9/Ntf3-coated beads.** We washed 100 μl of agarose beads (Affi-gel Blue gel, Bio-Rad Laboratories) three times with sterile water and four times with PBS. For coating the beads with Fgf9, we mixed 20 μl of bead solution with 10 μl of an Fgf9 solution (200 ng $\mu l^{-1}$) and incubated them overnight at 4 °C. As a control, the beads were coated with BSA; 20 μl of bead solution was mixed with 2 0 μl of BSA (1 mg $ml^{-1}$). Capillaries of appropriate nozzle size were prepared in a temperature-controlled pipette puller (PIP5, HEKA). E16.5–17.5 wild-type slices (200 μm-thick) were sectioned on a Leica vibratome and placed on cell-culture inserts inside a six-well plate (see above). Before placing the beads on the slices, we washed them twice with PBS and then resuspended them in 100 μl of slice culture medium. Using a mouth pipette, we picked beads of the desired size and placed them over the cortical plate. The cultured slices were fixed after two division rounds and immunostained (see above). For quantification of Olig2-positive cells, we first selected slices at similar levels along the rostrocaudal axis. An area of 440 × 293 μm was selected in the ventricular zone/SVZ and the cortical plate and the number of Olig2-positive cells in this region was quantified using ImageJ (an average of 822 cells in slices beaded with Fgf9 versus 182 cells in slices beaded with BSA). At least ten slices per condition were collected randomly from five wild-type embryos and analyzed.

**Cell-cycle measurement.** Cell-cycle measurement was carried out as described previously[47]. Briefly, pregnant mice were injected with IddU (<4 mg per kg) at $t = 0$ h to label S-phase cells. The same mice were injected with BrdU (20 mg per kg) at $t = 1.5$ h and the mice were killed at $t = 2$ h. Brains were isolated and processed as described above. We used mouse antibody to BrdU/IddU

(Chemicon, MAB3424, 1:55) and rat antibody to BrdU (Abcam, ab6326, 1:300). For secondary antibodies, we used Cy2-conjugated antibody to rat IgG (Jackson, 1:300) and AlexaFluor 555–conjugated antibody to mouse IgG (Invitrogen, 1:300). We counted double-labeled $S_{cells}$ (cells that are in the S-phase by $t = 2$ h and hence, labeled with both BrdU and IddU), single-labeled $L_{cells}$ (cells that left the cell cycle in the 1.5-h time interval and were labeled only with IddU) and total cell number, taking only the proliferating cell compartment of the neocortex into account. Cell-cycle length was calculated. *t* tests were performed using Sigmastat and graphs were made using Excel.

**Microarray analysis.** In the first series of arrays, we examined gene expression in neocortex and hippocampal tissue from two control (*Sip1*$^{loxP/+}$*; Nestin-cre*) and two mutant (*Sip1*$^{loxP/}$*; Nestin-cre*) E18.5 littermates, each taken from two different litters. In a separate experiment, we used E14.5 neocortex and hippocampal tissue from two control (*Sip1*$^{loxP/+}$*; Nex-cre*) and two mutant (*Sip1*$^{loxP/}$*; Nex-cre*) littermates. RNA from neocortex and hippocampus tissues was isolated using an RNeasy kit according to the manufacturer's protocol (Qiagen). The isolated RNA was inspected for integrity and purity using an Agilent Bioanalyzer and a NanoDrop spectrophotometer, respectively. All samples were of similar RNA quality. Starting with 1 μg of total RNA, we amplified RNA by *in vitro* transcription with a biotin labeling reaction (Amersham Biosciences). The probes were purified and analyzed again for yield (>20 μg) and purity (260:280 and 260:230 nm). We fragmented 10 μg of the resulting antisense RNA according to the manufacturer's protocols (Amersham Biosciences) and resuspended it in 260 μl of hybridization buffer.

Codelink Mouse Whole Genome array is a single array representing ~35,000 transcripts. The gene array chips were hybridized in a shaker-incubator at 37 °C at 300 rpm for 18 h and washed and stained with Cy5-streptavidin according to manufacturer's protocols (Amersham Biosciences). The Agilent DNA Microarray scanner was used for scanning and image analysis was performed with Codelink Expression Analysis 4.1 software (Applied Microarrays).

**Microarray data analysis.** Statistical data analysis was performed on the mean foreground and median background intensities, as provided by the Codelink Expression Analysis 4.1 software. Data analysis was performed in the R programming environment, in conjunction with the packages (the packages Codelink and Limma) developed in the Bioconductor project (http://www.bioconductor.org). All probes that were flagged as manufacturing spot removed, irregular or saturated by the Codelink Expression Analysis software were removed before the normalization. Data were background corrected; in case this resulted in a negative value, the background corrected intensity for that spot was set equal to 0.5. All data were normalized with quantile normalization and base 2 log-transformed. We omitted all probes that had less than two present calls (that is, flagged as good signal) over all samples. In this way, we retained 31,251 out of 36,227 spots.

The differentially expressed genes between the control samples and the *Sip1*|*Nestin* and *Sip1*|*Nex* samples were assessed via the Linear Models for Microarray Data (Limma), as described previously[48]. This allows one to fit a linear model to the expression data for each gene and applies an empirical Bayesian strategy to compute the gene-wise residual s.d. Thereby, the power of the test is increased, which is especially beneficial for smaller datasets. As the data had a strong litter effect, this was taken into account by estimating the average correlation in each litter[49]. To control the false discovery rate, we performed multiple testing correction and probes with a corrected *P* value smaller than 0.01 were selected[50].

**Qualitative PCR and ISH.** The expression of *Ntf3* and *Fgf9* mRNA was validated by quantitative PCR (ABI Prism 7000, Applied Biosystems) on E14.5 cDNA synthesized from mutant and control neocortex mRNA. *Ntf3*, *Fgf9*, *Fgfr2*, *Fgfr3* and *TrkC* mRNA was detected on brain slices (6 μm) by cold ISH using an automated platform (Ventana Discovery, Ventana Medical Systems; details of procedures can be obtained at request). The Fgf9 probe was a kind gift from D. Ornitz (Washington University), and the TrkC probe from L. Lei (UT Southwestern Medical Center). All other probes were cloned from PCR fragments using the PCR-Script Amp cloning kit (Stratagene).

**ChIP analysis.** *In silico* analysis of the *Ntf3* and *Fgf9* genes, including a 5,000-bp region upstream of the coding sequence, revealed several potential Sip1-binding sites. Qualitative PCR primers were designed (Vector NTi) to cover 500-bp regions 4 kb upstream of the first exon. For *Fgf9*, we also included regions covering Sip1 sites (fragments containing at least two CAC CT(G) half-sites separated by less than 100 bp) in the introns. The performance of these primers was first validated on an AbiPrism qualitative PCR platform using a dilution series of genomic DNA. Later, these primers were used to assess the quality of the sheared or enzymatically digested chromatin (input DNA). To prepare the chromatin, we dissected mouse neocortex and hippocampus tissue from E16.5–17.5 CD1 embryos in ice-cold Hank's solution, cut the tissue into smaller pieces, and dispersed and counted the cells. The whole-cell suspension was then cross-linked in 1% formaldehyde (vol/vol) for 10 min at 24 °C. Cross-linking was stopped by addition of glycine to a concentration of 0.125 M. After several washes with PBS, the cell pellet was dissolved in lysis buffer (5 mM PIPES (pH8.0), 85 mM KCl and 0.5% NP40, vol/vol) and kept on ice for 1–1.5 h to lyse the cells. The lysates were then passed 20 times through a 26G needle to release the nuclei. Nuclei were lysed in nuclear lysis buffer (50 mM Tris-HCl (pH 8.1), 10 mM EDTA, 1% SDS, wt/vol) for 10–15 min before shearing. Chromatin was sonicated eight times for 30 s in a Branson Sonifier 450 (power setting 3) and with a constant duty cycle to obtain chromatin fragments of 500 bp (mean size). Samples were cooled down for 1 min on ice between each pulse. An aliquot of the sheared chromatin was reverse-crosslinked and purified to check shearing efficiency and to measure DNA concentration. Samples were further processed according to the protocol provided with the ChiP-IT kit (Active Motif). For each immunoprecipitation reaction, 25 μg of chromatin was used. Immunoprecipitation was performed using 5 μg of crude rabbit antibody to Sip1 or 5 μg of rabbit IgG as a negative control (Abcam). After recovery of the Sip1-bound DNA fragments from the immunoprecipitation, fragments of *Ntf3* and *Fgf9* promoters were detected by qualitative PCR on 20 ng of DNA (immunoprecipitate) per sample in triplicate, using the validated primers described above. For each region, at least three independent immunoprecipitation reactions were carried out. Next, the relative enrichment of the bound versus the unbound regions (after ChIP with antibody to Sip1) was calculated relative to negative control rabbit IgG.

**Statistical analysis.** For all experiments, we used a *t* test to analyze the difference between two groups of data (see different subheadings). This analysis was performed using Microsoft Excel.


46. Polleux, F. & Ghosh, A. The slice overlay assay: a versatile tool to study the influence of extracellular signals on neuronal development. *Sci. STKE* 11 June 2002, l9.
47. Martynoga, B., Morrison, H., Price, D.J. & Mason, J.O. Foxg1 is required for specification of ventral telencephalon and region-specific regulation of dorsal telencephalic precursor proliferation and apoptosis. *Dev. Biol.* **283**, 113–127 (2005).
48. Smyth, G. Linear models and empirical bayes methods for assessing differential expression in microarray experiments. *Stat. Apple. Genet. Mol. Biol.* **3**, 3 (2004).
49. Smyth, G.K., Michaud, J. & Scott, H.S. Use of within-array replicate spots for assessing differential expression in microarray experiments. *Bioinformatics* **21**, 2067–2075 (2005).
50. Benjamini, Y. & Hochberg, Y. Controlling the false discovery rate: a practical and powerful approach to multiple testing. *J. R. Stat. Soc. Series B Stat. Methodol.* **57**, 289–300 (1995).





doi:10.1038/nn.2409